Organic Geochemistry 87 (2015) 68–77

Contents lists available at ScienceDirect

Organic Geochemistry

journal homepage: www.elsevier.com/locate/orggeochem

Compound-specific carbon isotope study on the hydrocarbon biomarkers in lacustrine source rocks from Songliao Basin

Li Wang [a,*], Zhiguang Song [a], Xinxing Cao [a,b], Yan Li [a,b]

[a] State Key Laboratory of Organic Geochemistry, Guangzhou Institute of Geochemistry, Chinese Academy of Sciences, Guangzhou 510640, China
[b] University of Chinese Academy of Sciences, Beijing 100049, China

ARTICLE INFO

Article history:
Received 17 April 2015
Received in revised form 23 July 2015
Accepted 29 July 2015
Available online 5 August 2015

Keywords:
Molecular markers carbon isotopes
Chemocline
Paleoenvironment
Upper Cretaceous
Nenjiang Formation

ABSTRACT

Stable carbon isotopic composition of organic matter ($\delta^{13}C_{org}$) and compound-specific $\delta^{13}C$ values of biomarkers from 15 lacustrine source rocks were analyzed to identify the original paleoenvironment and source organisms. The $\delta^{13}C$ values of hopanes ($\delta^{13}C_{hop}$) ranged from −68.7‰ to −32‰ and exhibit strongly ^{13}C-depleted values in the lower part of Member 1 of the Nenjiang Formation (K_2n^1, up to −68.7‰), suggesting an origin from predominantly methanotrophic bacteria. ^{13}C-enriched $\delta^{13}C_{Ga}$ values and significantly ^{13}C-depleted $\delta^{13}C_{hop}$ in K_2n^1, which coincide with water stratification and an intermittent anoxic photic zone, represents a shallow chemocline. The presence of an intermittent anoxic photic zone, which means that the anoxia expanded into the euphotic zone, is beneficial for OM preservation and results in high values of TOC and HI in this section. However, the absence of gammacerane and ^{13}C-enrichment of $\delta^{13}C_{hop}$ in Member 2 of Nenjiang Formation (K_2n^2) reflect a deeper chemocline, corresponding to relatively oxidizing conditions and low values of TOC and HI. Moreover, the negative correlation of TOC vs $\delta^{13}C_{org}$ and HI vs $\delta^{13}C_{org}$ reflects the control of OM formation by sedimentary environments rather than productivity in the water column. Thus, the depth of the chemocline not only controls the abundance of OM but also affects the development of the microbial community, such as chemoautotrophic bacteria in the deep chemocline and chemoautotrophic and methanotrophic bacteria in the shallow chemocline. Moreover, $\delta^{13}C_{Ga}$ and $\delta^{13}C$ values for 4-methyl steranes are related to water salinity, with a higher salinity accompanied by ^{13}C-enrichment in gammacerane and 4-methyl steranes.

1. Introduction

The Songliao Basin is the largest Mesozoic continental sedimentary basin in China. It contains a continuous series of Cretaceous lacustrine strata and therefore preserves valuable information related to the paleontology, paleoclimate and paleoenvironmental conditions of the basin, which are very important to understanding the geology of Cretaceous continental strata and global climate change.

The depositional environments and source of organic matter (OM) in Songliao source rocks has been extensively studied (Yang et al., 1981; Huang et al., 1998; Feng et al., 2009, 2011; Chamberlain et al., 2013). Prior studies have shown that the Qiangshankou and Nenjiang Formations, the two major sets of OM-rich source rocks, were deposited in a deep freshwater lake, but under eutrophic and anoxic conditions (Wang et al., 2011; Bechtel et al., 2012; Song et al., 2013). Nevertheless, Hou et al. (2000) suggested that the massive hydrocarbon source rocks were developed under brackish–saline conditions and may be associated with marine transgressions. Recently, new lines of evidence regarding marine transgressions from fossils and sulfur geochemistry have been reported (Xi et al., 2011; Huang et al., 2013). Existing investigations reveal that the sedimentary environments are more complex and spatially heterogeneous (Wang et al., 2011; Bechtel et al., 2012). However, we still do not clearly understand the relationship between sedimentary environments and OM sources during the period of the deposition of the massive lacustrine source rocks in the Songliao Basin, such as the water stratification stability, depth of chemocline, and aqueous CO_2 circulation as well as the effects of microorganisms. Besides, there are few papers involving the relationship between redox conditions and biological disturbance in the lacustrine sedimentary.

Biomarker distributions, together with their carbon isotopic compositions, can provide insights into the composition of the biota in the original depositional environments (Hayes et al., 1990; Grice et al., 1998; Koch, 1998; Sepúlveda et al., 2009). The

* Corresponding author at: 511 Kehua St., Tianhe, Guangzhou, Guangdong, China. Tel.: +86 20 85290186.
E-mail address: wangli@gig.ac.cn (L. Wang).

http://dx.doi.org/10.1016/j.orggeochem.2015.07.011
0146-6380/

present work complements previous geochemical studies by using a stable carbon isotopic approach at the molecular level. In this study, we analyzed the $\delta^{13}C_{org}$ and molecular carbon isotope compositions of the biomarkers based on a closely sampled profile from the Nenjiang Formation in the Songliao Basin. Here we aim to unravel the relationship between the depositional paleoenvironment and original organisms using molecular carbon isotopes of biomarkers.

2. Geological setting and experimental procedures

The Songliao Basin, located in the northeast of China, is a continental sag basin with late Paleozoic and early Mesozoic consolidated crust as the basement. There have been several expansions and contractions of the Songliao paleo-lake (Feng et al., 2010). There were at least five large lacustrine transgressions during basin development, and each time the lacustrine transgression formed a massive dark mudstone or oil shale. Specifically, during the deposition of K_2n^1 and K_2n^2, a wide semi-deep and deep water lacustrine depositional system rapidly developed in the Songliao Basin and covered an area exceeding 2×10^5 km^2 (Feng et al., 2010). In this paper, samples were collected from depths of 950 m to 1300 m in the "SK-1" borehole, covering the whole section of the K_2n^1 and the lower part of the K_2n^2 (Fig. 1). A total of 15 source rocks have been extracted, and some of them have been sampled for organic carbon isotope analysis and molecular carbon isotope measurement.

The samples were crushed to 100 mesh and Soxhlet extracted using a mixture of CH_2Cl_2 and MeOH (9:1, v/v). The extracts were initially dissolved in hexane to remove asphaltenes, and the maltene fraction was separated into aliphatic, aromatic and polar fractions via alumina/silica gel column chromatography using hexane, a mixture of hexane and CH_2Cl_2 (4:1, v/v), and a mixture of CH_2Cl_2 and MeOH (1:1, v/v), respectively. The saturated fractions were further separated into *n*-alkanes and branched/cyclic fraction by urea adduction and then analyzed by GC–MS and GC-isotope ratio MS.

HCl was used to remove carbonates from the powdered samples, and then the residual powder was wrapped with a tinfoil sheet. After that, the samples were analyzed for the carbon isotope composition of OM using a Finnigan DELTA plus XL elemental mass spectrometer. Each sample was measured at least twice to ensure the isotopic error of parallel analyses was < 0.5‰.

The total organic carbon (TOC) content was measured by standard pyrolysis using a Rock–Eval 6 (Vinci Technologies) and was calculated as the combination of discharged CO below 570 °C and released CO_2 below 400 °C.

A Thermo Finnigan gas chromatography mass spectrometer (GC–MS) was used for specific biomarker analysis, using an electron impact ion source at 70 eV. A J&W DB-5 fused silica column (30 m × 0.25 mm i.d × 0.25 μm film thickness) was used. The

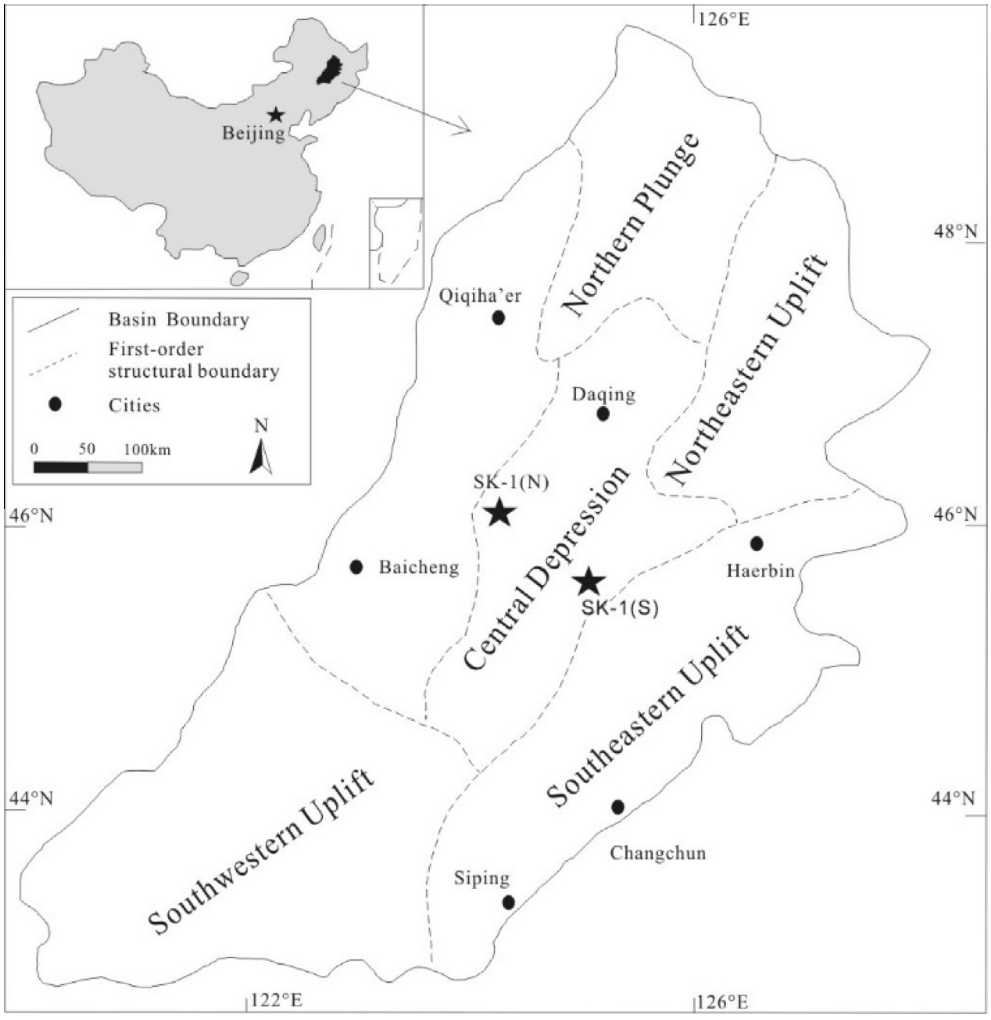

Fig. 1. SK-1 drilling sites in the Songliao Basin, China.

injector and detector temperatures were 290 °C and 300 °C, respectively. The samples were injected in splitless mode, and N_2 was the carrier gas. The oven temperature was initially 80 °C (held for 2 min) and was then programmed at 4 °C/min to 290 °C (held for 20 min).

The branched/cyclic fractions were analyzed using a GV IsoPrime GC–ir–MS with a DB-1 column to detect their molecular carbon isotopic values. Samples were injected in splitless mode. For *n*-alkane analyses, a GC oven was programmed from 80 to 290 °C at 4 °C/min and held isothermally at 80 °C for 2 min and at 290 °C for 20 min. For branched/cyclic fraction analysis, the GC oven was operated as follows: 80 °C (held 2 min) to 245 °C at 1 °C/min, then to 290 °C at 10 °C/min (held 10 min). Each sample was analyzed at least twice, and the standard deviations of the replicates were calculated for each *n*-alkane to estimate reproducibility. The standard carbon isotope gas was calibrated using the NS22 crude oil standard provided by IAEA; the isotopic error of parallel analyses was < 0.5‰.

3. Results and discussion

3.1. Basic geochemical parameters

The T_{max} values in K_2n^{1+2} are lower than 440 °C, Ts/Tm are approximately 0.2, and 22S/(22S + 22R) of C_{31} hopane ratios are < 0.5, indicating an immature to low mature stage in these samples. These parameters vary slightly over the whole profile, but indicate a similar maturity for each sample. In other words, the variation of the biomarker parameters and the carbon isotopic values in profile are not due to thermal maturity.

According to the depth variation of total organic matter (TOC), hydrogen index (HI) and pristane/phytane (Pr/Ph), the whole profile can be divided into four sections (Table 1). Section I is the bottom part of the K_2n^1 member from a depth of 1116–1126 m. It has a high value of TOC (3.6–9.2%) and HI, but a large fluctuation of Pr/Ph. The carbon isotopic values for pristane ($\delta^{13}C_{pr}$) and phytane ($\delta^{13}C_{ph}$) were ca. −31.5‰. The carbon isotopic composition of steranes varies from −32.5‰ to −27.9‰, and the $\delta^{13}C_{hop}$ varies from −40.6‰ to −25.9‰.

Section II covers the 1099–1116 m interval of the K_2n^1 member and is characterized by a high Pr/Ph and the lowest TOC content (0.24–0.84%) in the profile. Due to the low content of OM, the $\delta^{13}C$ values of steranes and hopanes were not measured in this section.

Section III contains the most important OM-rich source rocks of the Nenjiang Formation and covers most of the middle to lower part of the K_2n^1 section, ranging from 1016 m to 1099 m. This section is characterized by high values of TOC and HI as well as a low Pr/Ph, with little variation. The $\delta^{13}C_{pr}$ and $\delta^{13}C_{ph}$ values are −32.4‰ and −32.1‰, respectively. Both C_{27} 5α-sterane and C_{29} 5α-sterane have similar carbon isotopic compositions, yet the C_{28} 5α-sterane is lower than the former by approximately 1‰. The $\delta^{13}C$ values of C_{28} 4α-methyl sterane and C_{29} 4α-methyl sterane are primarily from −35‰ to −30‰, but the $\delta^{13}C$ of the C_{30} 4α-methyl sterane is clearly ^{13}C-enriched ranging from −30‰ to −20‰. As for hopanes, most of them are ^{13}C-depleted varying from −70‰ to −30‰; only the $\delta^{13}C_{Ga}$ value is ^{13}C-enriched.

Section IV ranges from 950 m to 1016 m, covering the entire lower part of the K_2n^2. This section is largely characterized by a gradual decrease in TOC and HI, along with a high ratio of Pr/Ph. C_{27}–C_{29} 5α-steranes and C_{28} and C_{29} 4α-methyl steranes have similar carbon isotopic compositions of approximately −32‰, while the C_{30} 4α-methyl sterane is relatively ^{13}C-enriched and varies from −29‰ to −25‰. Most of the hopanes vary in this interval from −45‰ to −32‰. Fig. 2 shows that all of the carbon isotopic compositions of the biomarkers have less fluctuation in section IV than in sections I and III; the $\delta^{13}C$ values of hopanes especially show a smaller variation range in section IV than in the other sections.

3.2. Stable carbon isotopic composition of biomarkers and ancient producers

3.2.1. Acyclic isoprenoids

Pristane and phytane originate from the photosynthetic products of algae and cyanobacteria, which represent primary producers in the water ecosystem (Hayes et al., 1990). In addition, pristane can also come from vitamin E (tocopherols), as well as methanogens, and halophilic bacteria can also generate phytane (Peters et al., 2005; Sepúlveda et al., 2009). Therefore, the $\delta^{13}C_{pr}$ and $\delta^{13}C_{ph}$ can verify their parent material. The $\delta^{13}C_{pr}$ and $\delta^{13}C_{ph}$ in K_2n^{1+2} are both approximately −32‰, indicating that they have a common origin. Compared to $\delta^{13}C_{org}$, $\delta^{13}C_{pr}$ is depleted in ^{13}C by 4‰ to 6‰, which accords with the relationship between the carbon isotope distributions of lipids and total OM (Hayes, 1993; Schouten et al., 1998). Accordingly, the pristane and phytane in these samples are mainly from photosynthesizing primary producers or heterotrophic organisms feeding on primary producers.

3.2.2. Steranes

The abundances of steranes are clearly lower than hopanoids in the samples (Fig. 3). We noticed that the relative abundance of 4α-methyl steranes in some samples is similar to that of the regular steranes. Previous studies have suggested that when steranes, pristane and phytane come from primary producers (such as algae and photosynthetic bacteria), their carbon isotope compositions will be very close to each other (Freeman et al., 1990; Collister et al., 1992; van Kaam-Peters et al., 1997). The $\delta^{13}C$ of C_{27} 5α-sterane and C_{29} 5α-sterane are close to $\delta^{13}C_{pr}$ and $\delta^{13}C_{ph}$, suggesting that they originate from the same algal species (Volkman, 2003; Peters et al., 2005). In K_2n^2, the $\delta^{13}C$ of the C_{28} 5α-sterane is clearly more negative by 2‰ than the $\delta^{13}C$ values of the C_{27} and C_{29} 5α-steranes. Previous studies suggest that the ancient producer of C_{28} 5α-sterane lived in the bottom of the aerobic zone (Zhang et al., 2012), so it could partly use OM-degraded CO_2 as a carbon source, even when atmospheric dissolved CO_2 was still the main carbon source.

A series of C_{28}–C_{30} 4α-methyl steranes have been identified. It is generally believed that 4α-methyl steranes are formed from the 4α-methyl sterols from dinoflagellates (Peters et al., 2005). Previous studies consider that water salinity can affect the distribution of 4-methyl sterane homologues. In our study, the C_{30} 4α-methyl sterane is the most abundant and C_{28} 4α-methyl sterane is the next most abundant. As shown in Fig. 4, the $\delta^{13}C$ values of C_{28} and C_{29} methyl steranes are approximately −31‰, indicating that they originate from a primary producer that lived in the upper photic zone. However, the $\delta^{13}C$ values of C_{28} and C_{29} 4α-methyl steranes show a significant negative excursion at the depth of 1063 m to 1051 m (Fig. 4), which may be related to massive freshwater input in a short time (unpublished hydrogen isotopic data) (Zhao et al., 2014). Relative to the C_{28} and C_{29} 4α-methyl steranes, the C_{30} 4α-methyl sterane is clearly enriched in ^{13}C, which may reflect the variation in water salinity. Especially in section III, the C_{30} methyl sterane is generally ^{13}C-enriched by about 5‰. The good positive correlation between the $\delta^{13}C$ value of the C_{30} 4α-methyl sterane and Ga/HopC_{31}R indicates that the $\delta^{13}C$ value of C_{30} 4α-methyl sterane can reflect the variation in water salinity (Fig. 5).

Table 1
TOC, Rock–Eval data, biomarker ratios and $\delta^{13}C_{org}$ values.

Section	Depth (m)	TOC (wt.%)	HI	T_{max} (°C)	Pr/Ph	Ts/Tm	C_{31} 22S/(22S + 22R)	Ga/HopC_{31}R	MTTCI	$^{13}C_{org}$ (‰)
IV	955.4	0.96	184	438	1.97	0.14	0.40	–	0.82	−25.91
	957.0	1.03	177	434	1.15	0.20	0.44	0.36	0.86	−26.17
	971.3	1.67	181	436	1.72	0.11	0.47	–	0.87	−25.65
	978.2	1.89	249	436	1.96	0.28	0.46	–	0.88	−26.82
	983.9	2.27	356	433	1.98	0.44	0.48	–	0.86	−26.62
	989.9	1.60	260	437	1.75	0.46	0.47	–	0.87	−26.99
	1001.4	2.34	422	435	2.24	0.36	0.50	–	0.83	−27.88
	1007.2	2.13	455	439	2.92	0.45	0.47	–	0.86	−29.12
	1012.6	3.66	623	445	2.49	0.44	0.47	–	0.83	−28.58
III	1016.8	4.95	727	439	0.92	0.66	0.54	0.78	0.79	−29.56
	1021.4	4.34	715	437	1.05	0.16	0.48	–	0.90	−28.33
	1028.7	1.36	475	436	0.65	0.21	0.49	0.79	0.64	−29.81
	1034.0	2.14	491	437	0.66	0.24	0.47	2.39	0.16	−29.36
	1039.0	2.98	603	437	0.74	0.24	0.44	0.78	0.24	−29.32
	1045.2	3.98	718	439	0.70	0.19	0.48	1.58	0.33	−29.46
	1051.0	4.45	680	439	0.76	0.13	0.51	0.96	0.91	−30.63
	1058.0	1.57	440	430	0.72	0.18	0.51	1.62	0.61	−27.67
	1061.1	2.58	599	433	0.81	0.21	0.49	0.53	0.69	−28.72
	1063.9	4.07	711	434	0.96	0.20	0.50	0.53	0.56	−29.09
	1066.7	3.09	652	437	0.75	0.22	0.51	0.75	0.64	−28.77
	1069.6	5.72	762	438	0.90	0.25	0.50	0.42	0.76	−29.85
	1072.4	3.71	688	437	0.64	0.22	0.51	1.20	0.51	−29.38
	1075.2	4.14	712	446	0.76	0.21	0.50	0.75	0.63	−29.57
	1078.0	3.45	677	447	0.64	0.21	0.51	1.08	0.59	−29.91
	1080.6	3.10	704	434	0.56	0.18	0.51	2.08	0.62	−29.56
	1083.3	6.43	647	433	0.59	0.18	0.49	0.95	0.44	−30.56
	1086.0	2.22	477	440	0.73	0.30	0.54	3.96	0.67	−29.09
	1092.0	5.70	812	444	0.46	0.25	0.53	1.66	0.70	−30.32
	1094.5	12.00	806	438	0.62	0.21	0.51	0.21	0.58	−29.40
	1097.5	2.79	544	437	0.60	0.21	0.53	0.93	0.66	−28.37
II	1099.5	0.24	75	437	1.24	0.18	0.55	–	1.00	−26.40
	1103.7	0.36	144	442	1.60	0.05	0.59	–	1.00	−27.16
	1107.1	0.53	164	442	1.85	–	0.52	–	1.00	−27.95
	1110.9	0.84	455	448	1.30	0.51	0.56	0.86	1.00	−30.59
I	1116.9	4.05	566	439	1.39	0.38	0.53	0.29	0.64	−29.65
	1118.4	0.16	–	438	2.78	0.24	0.53	0.21	0.65	–
	1121.4	5.45	587	438	2.36	0.41	0.53	0.25	0.47	–
	1122.7	4.35	649	442	0.88	0.15	0.55	2.09	0.21	−28.48
	1123.2	7.01	766	442	1.05	0.25	0.54	0.53	0.34	–
	1124.3	7.97	737	443	0.80	0.19	0.54	0.76	0.31	–

3.2.3. Hopanoid compounds

Hopanes are derived from the cytomembrane of prokaryotic bacteria, including cyanobacteria, heterotrophic bacteria, methanotrophic bacteria and chemoautotrophic bacteria (Sinninghe Damsté and Schouten, 1997). Therefore, the ratio of hopanes to steranes (Hop/Ste) can reflect the relative contribution between bacteria and algae. The Hop/Ste values are high in K_2n^2, suggesting strong bacterial degradation and poor preservation of steranes due to aerobic conditions (Boreham et al., 1994). Although the relative abundance of steranes is higher in K_2n^1, the content of hopanes is still greater than the steranes (Fig. 3). Thus, the abundant hopanes indicate that bacteria were quite numerous in the lacustrine sediments, which is significantly different from marine deposition (Ourisson et al., 1979; Peters et al., 2005).

The $\delta^{13}C_{hop}$ in K_2n^1 cover the large interval from −32‰ to −68.7‰ (Fig. 2). When the source of hopanes is chemoautotrophic bacteria, the $\delta^{13}C_{hop}$ range from −34‰ to −45‰ (Freeman et al., 1990; Collister et al., 1992). Due to use of ^{13}C-depleted CO_2 as a carbon source, these OM are much lighter than those formed by primary producers (Huang et al., 1995; Schouten et al., 2000). Additionally, the more ^{13}C-depleted hopanes are considered to result from methanotrophic bacteria (Freeman et al., 1990; Collister et al., 1992; Grice et al., 2001; Schouten et al., 2001), which have been reported in many lacustrine source rocks (Freeman et al., 1990; Collister et al., 1992) and modern lacustrine ecosystems (Neunlist et al., 2002). In the lower part of section III, the $\delta^{13}C_{hop}$ are strongly ^{13}C-depleted (down to −68.7‰), suggesting a methanotrophic bacterial input (Schouten et al., 2001; Volkman et al., 2015). However, in sections I, II and the upper part of section III, the values are mostly greater than −45‰, indicating that chemoautotrophic bacteria dominate. The $\delta^{13}C_{hop}$ are ^{13}C-enriched in K_2n^2 relative to K_2n^1, revealing that their sources are chemoautotrophic bacteria rather than methanotrophic bacteria. Although bacteria were more abundant in K_2n^2 than in K_2n^1 in terms of Hop/Ste values, the $\delta^{13}C_{hop}$ values are more ^{13}C-depleted in K_2n^1, which may imply that there are more anaerobic microbes in the reducing environments of K_2n^1 than in the oxic environments in K_2n^2.

Based on the $\delta^{13}C$ values of biomarkers in K_2n^1, the OM sources are aquatic organisms, predominantly with abundant chemoautotrophic bacteria and with limited methanotrophic bacteria. During the deposition of K_2n^2, lower algae and bacteria are the dominant sources, as land plant input increased and aquatic organisms decreased.

3.3. Carbon isotopic composition of OM ($\delta^{13}C_{org}$)

As shown in Fig. 6, $\delta^{13}C_{org}$ is relatively ^{13}C-depleted in section III, with an average value of −29.4‰. These sections are consistent with the low values of Pr/Ph and high TOC and HI values. However, in sections IV, the Pr/Ph values are high, TOC and HI are low, and $\delta^{13}C_{org}$ is clearly enriched in ^{13}C, with an average of −26.9‰. Previous studies showed that in shallow chemocline environments, $\delta^{13}C_{org}$ values are low and constant, but are relatively enriched and

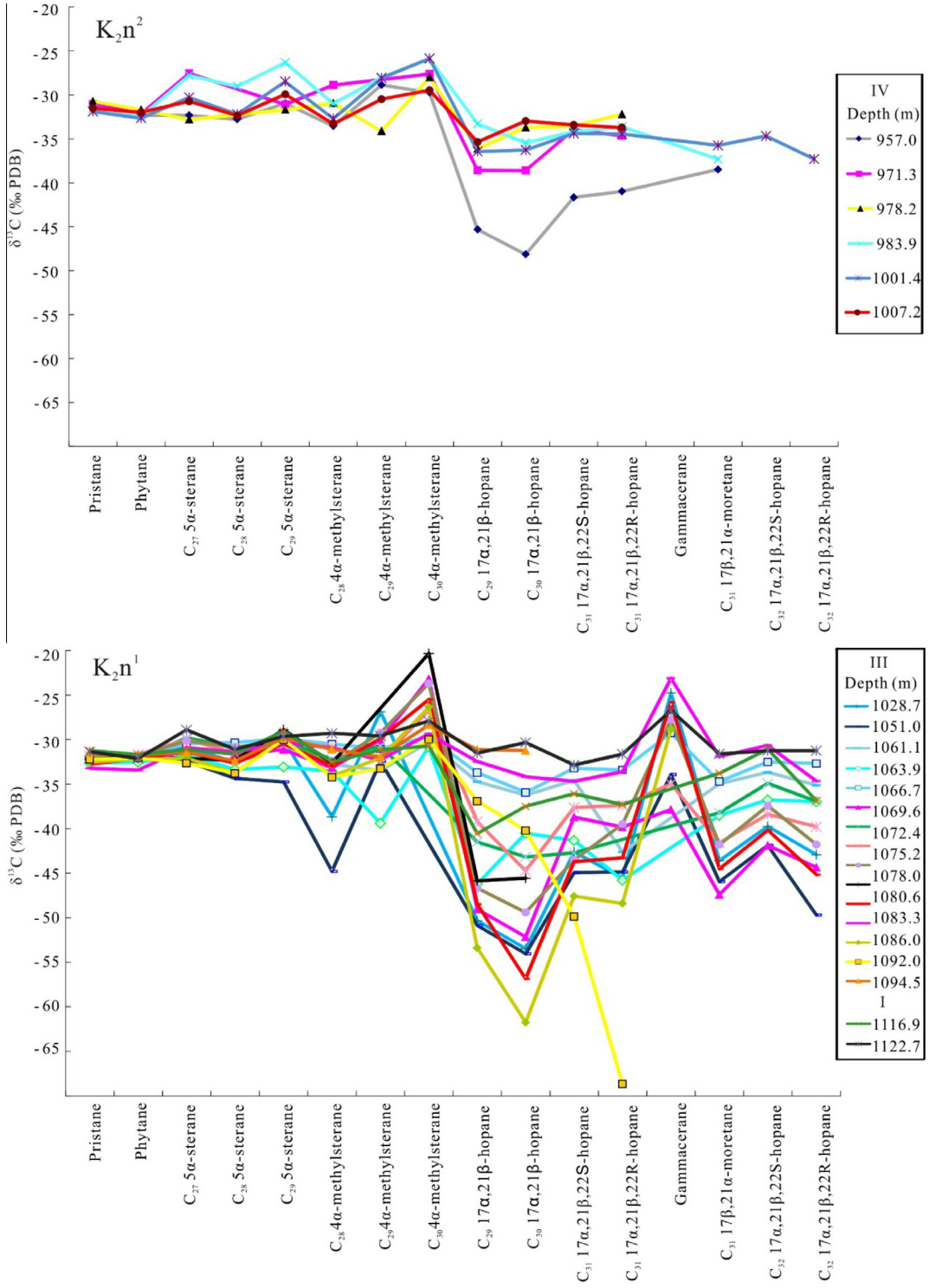

Fig. 2. Distributions of molecular carbon isotope values for selected biomarkers.

more variable in deep chemocline environments, probably due to the significant contributions of OM produced by chemoautotrophic and/or anaerobic photoautotrophic microbes in deeper environments (Luo et al., 2014). As mentioned before, there are more anaerobic microbes in the reducing environments of K_2n^1 (discussed in detail below). On the one hand, the bacteria tend to break down the OM and use up the oxygen, which provides ^{13}C-depleted CO_2. On the other hand, the OM produced by the anaerobic bacteria is much more depleted in ^{13}C. Furthermore, the anoxic conditions increased the preservation potential of OM. Thus, all of these factors make the $\delta^{13}C_{org}$ values in anoxic environments lower by ca. 3‰ than in aerobic conditions.

Furthermore, there is a good negative correlation of TOC vs $\delta^{13}C_{org}$ and HI vs $\delta^{13}C_{org}$ (Fig. 7). It is commonly thought that concentrations of CO_2 in water can reflect the productivity of the aquatic environment (Schouten et al., 2000). When productivity rises, the CO_2 content in water becomes gradually restricted, which leads to ^{13}C-enriched $\delta^{13}C_{org}$. This process is eventually manifested in

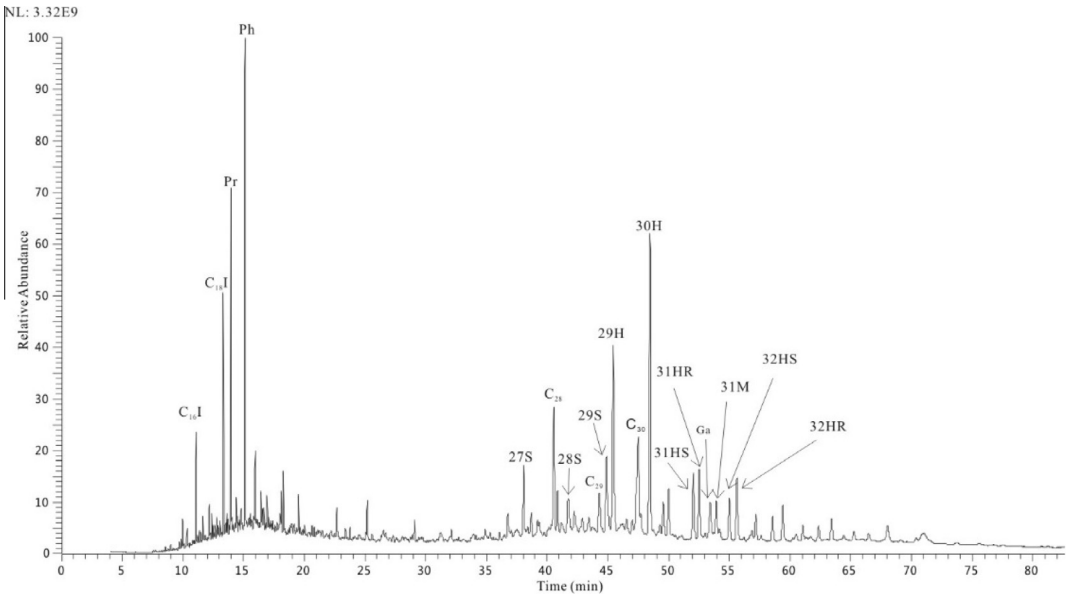

Fig. 3. Total ion chromatogram for branched/cyclic fraction from 1083.3 m depth sample showing the distributions of isoprenoids (C_{16} isoprenoid (C_{16}I), C_{18} isoprenoid (C_{18}I), pristane (Pr), phytane (Ph)), C_{27} 5α-sterane (27S), C_{28} 4α-methylsterane (C_{28}), C_{28} 5α-sterane (28S), C_{29} 4α-methylsterane (C_{29}), C_{29} 5α-sterane (29S), C_{29} 17α,21β-hopane (29H), C_{30} 4α-methylsterane (C_{30}), C_{30} 17α,21β-hopane (30H), C_{31} 17α,21β,22S-hopane (31HS), C_{31} 17α,21β,22R-hopane (31HR), Gammacerane, C_{31} 17β,21α-moretane (31 M), C_{32} 17α,21β,22S-hopane(32HS), C_{32} 17α,21β,22R-hopane (32HR).

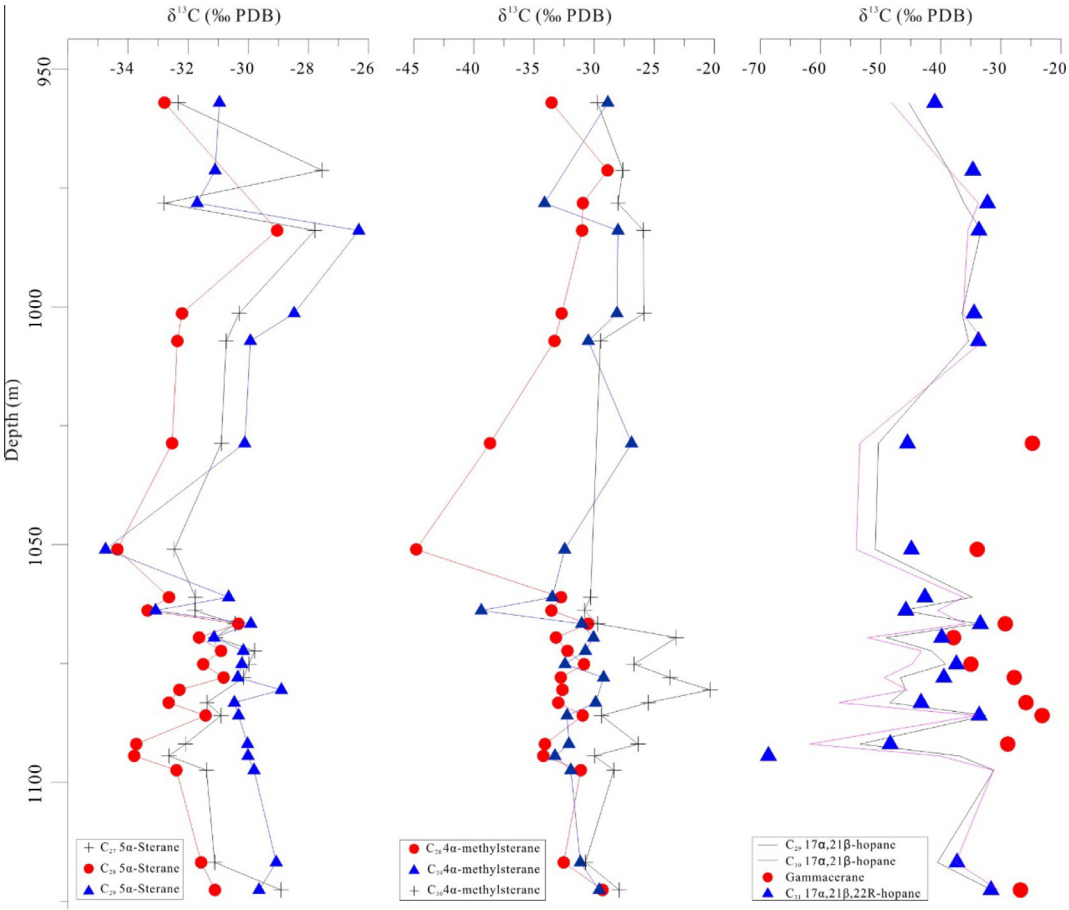

Fig. 4. Variation in molecular carbon isotope values for steranes, hopanes and gammacerane.

TOC and $\delta^{13}C_{org}$ having a significant positive correlation (Curiale and Gibling, 1994). As discussed previously, the productivity of the aquatic environment is quite high during the deposition of K_2n^{1+2}. However, the correlation between TOC and $\delta^{13}C_{org}$ is

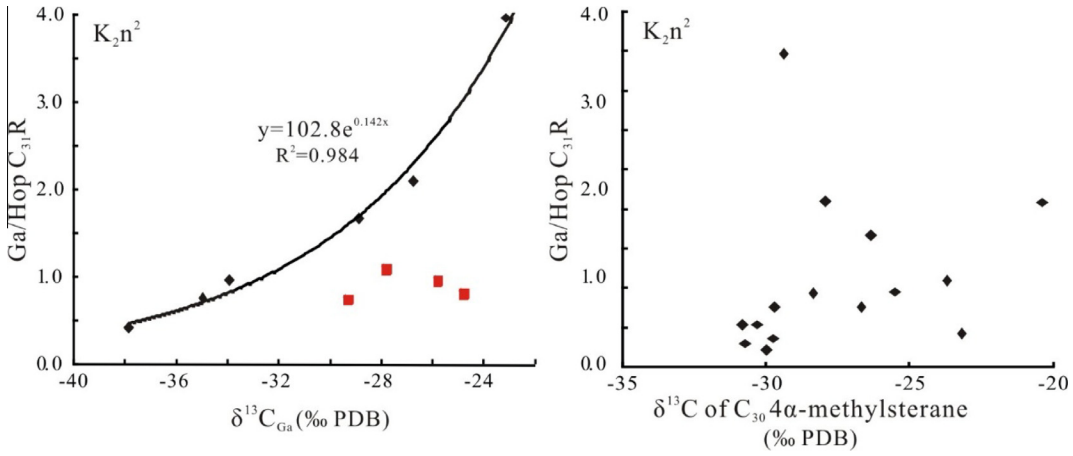

Fig. 5. Correlations of Ga/HopC_{31}R vs $\delta^{13}C_{Ga}$ and Ga/HopC_{31}R vs $\delta^{13}C$ of C_{30} 4-methyl sterane. Ga = gammacerane; HopC_{31}R = C_{31} 20R-homohopane.

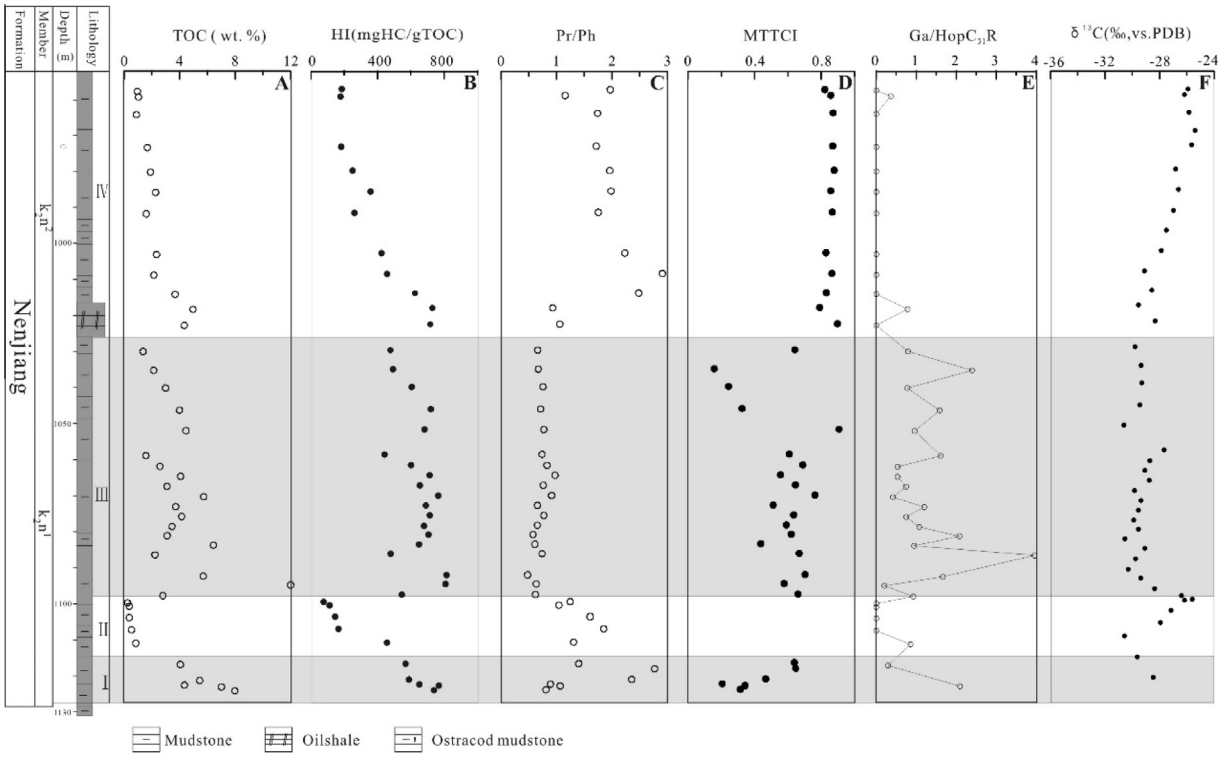

Fig. 6. Variation of TOC, HI, Pr/Ph, MTTCI, gammacerane index and $\delta^{13}C_{org}$. (A and B) Abundance of total organic carbon and hydrogen index (results from Rock–Eval). (C) Variation of pristane vs phytane ratio can reflect the relative redox condition. (D) α-/total-methyltrimethyltridecyl chromans (MTTCs) can indicate paleo-salinity from Wang et al. (2011). (E) Gammacerane index (Ga/HopC_{31}R), an an indicator of water stratified and salinity from Song et al. (2013). (F) Variation of $\delta^{13}C_{org}$. The average value is −26.9‰ in IV and −29.4‰ in III section, respectively.

negative instead of positive. In addition, the study of the Fort Worth Basin also reported the same correlation: decreasing $\delta^{13}C_{org}$ along with increasing TOC, which is interrelated with water stratification and anoxic conditions due to sea level rise within the basin. Therefore, we speculate that $\delta^{13}C_{org}$ in our study is mainly controlled by the sedimentary environment. The salinity stratified water column with anoxic conditions in the deep water are not only good at forming enormous amounts of OM but also provide favorable conditions for the preservation of OM, which causes high TOC values and ^{13}C-depletion of $\delta^{13}C_{org}$, and vice versa. So the negative correlation of TOC vs $\delta^{13}C_{org}$ and HI vs $\delta^{13}C_{org}$ in Songliao organic source rocks were the result of a complex interplay among basin anoxia and biological effects. Meanwhile, the $\delta^{13}C_{org}$ values in Songliao lacustrine sediments are more depleted in ^{13}C than the $\delta^{13}C_{org}$ values of contemporaneous lacustrine sediments from Russia and Japan (Hasegawa, 1997; Hasegawa et al., 2003), which may be related to microorganisms flourishing in the Songliao paleo-lake, implying that there is recycling of endogenous nutrients and CO_2 by primary producers (Meyers and Ishiwatari, 1993).

3.4. Sedimentary environments and biological effects

Previous studies suggested that there was a stable water salinity stratification in K_2n^1, especially in the lower part of the K_2n^1

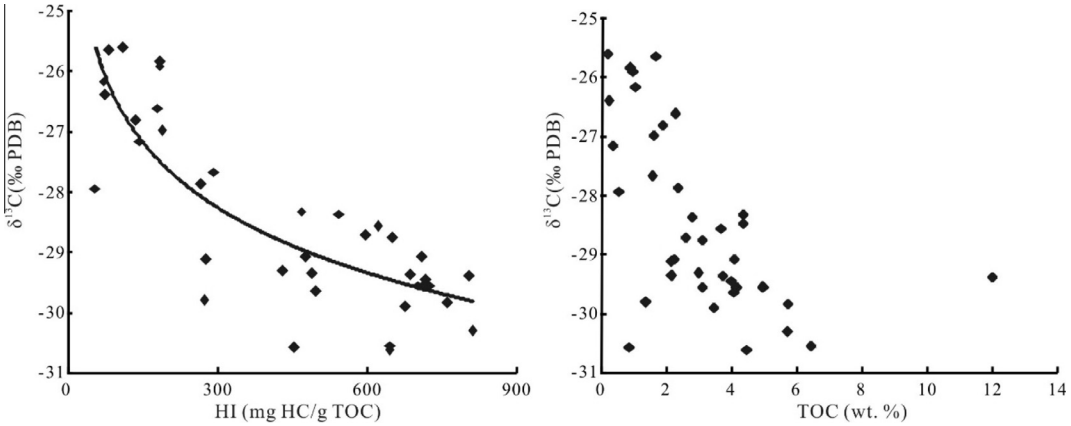

Fig. 7. Correlations of HI vs $\delta^{13}C_{org}$ and TOC vs $\delta^{13}C_{org}$.

member and even the existence of intermittent photic zone anoxia. Photic zone anoxia refers to an anoxic layer that has expanded up to the euphotic zone (Summons and Powell, 1986), resulting in shallow chemocline environments. A chemocline (redox interface) separates the upper aerobic water from bottom anoxic water. The upper layer is an aerobic freshwater environment, while the lower layer is anoxic brackish to saline water (Wang et al., 2011). In K_2n^2, the water stratification was destroyed along with the aerobic and brackish water environments. According to the $\delta^{13}C_{hop}$, chemoautotrophic bacteria and methanotrophic bacteria flourished in K_2n^1, while chemoautotrophic bacteria dominated in K_2n^2, especially in the intermittent photic anoxia zone, which may be related to the different environments of K_2n^1 and K_2n^2. OM decomposition consumes a large amount of oxygen to form CO_2, and water stratification inhibits the access of oxygen from the upper layer to lower water, which makes the lower water more anoxic and leads to decomposition products being further degraded into CH_4, H_2 and H_2S under anaerobic conditions (Cabrera et al., 2002). Especially under the shallow chemocline condition, more reducing gases were generated and partially dissolved in water and then utilized by methanotrophic and other anaerobic bacteria (e.g., green sulfur bacteria). Because of the absence of water stratification in K_2n^2, upper oxygen could easily access the bottom water, resulting in more OM decomposition into plentiful CO_2. This CO_2 can be used by chemoautotrophic bacteria as a carbon source, which resulted in the prevalence of chemoautotrophic bacteria in K_2n^2.

Additionally, the OM derives from many sources, not only from ancient primary producers but also from consumers and secondary producers (Freeman et al., 1990; Schaffner and Swart, 1991). Some types of microorganism use carbon sources with very specific ^{13}C signals or have a metabolism that results in characteristic isotopic ratios. Thus their isotopic signatures can then be used to identify their ancient producers (including primary and secondary producers). For example, gammacerane is commonly considered to be derived from tetrahymanol which originates from a type of bacteria-consuming ciliate living in the interface of the chemocline (Sinninghe Damsté et al., 1995; Peters et al., 2005). The $\delta^{13}C_{Ga}$ values cover a wide interval, from −37.9‰ to −23.9‰ (Fig. 2). There is a good positive correlation between $\delta^{13}C_{Ga}$ and the gammacerane index ($Ga/HopC_{31}R$), and the correlation coefficient reached 0.98, indicating that the water salinity has a significant influence on $\delta^{13}C_{Ga}$ values (Fig. 5): higher water salinity leads to ^{13}C-enrichment of $\delta^{13}C_{Ga}$. However, according to the formula, four samples are heavier by 6‰ to 10‰ than the corresponding $\delta^{13}C_{Ga}$ values under relevant salinity conditions, which suggests that the $\delta^{13}C_{Ga}$ value is not only controlled by water salinity but also the food source of its biological precursor (Michael and Samuel, 1978). Referring to the production of a bacteria-consuming organism, the $\delta^{13}C$ value of gammacerane ($\delta^{13}C_{Ga}$) can reflect the $\delta^{13}C$ value of the ciliates' food. When ciliates prey on green sulfur bacteria (which is ^{13}C-enriched by approximately 16‰), then its metabolic product (gammacerane) will consequently be enriched in ^{13}C. Previous studies suggested that the abundant aryl isoprenoid and isorenieratane detected in the lower part of K_2n^1 illustrates the existence of green sulfur bacteria during an intermittent photic anoxia period (Bechtel et al., 2012; Song et al., 2013), which corresponds to the period of ^{13}C-enriched $\delta^{13}C_{Ga}$ values.

Finally, Pedersen and Calvert (1990) emphasized the influence of high productivity on high OM deposition (Pedersen and Calvert, 1990). They believed that the anaerobic environment of OM-rich areas is due to high productivity caused by dissociation oxygen being exhausted in bottom water, and the anaerobic environment itself is not the cause of the OM-rich deposition. Thus, the massive black shale sedimentation during the Cretaceous period is also associated with the high productivity of the ocean rather than the anoxic event itself. Previous evidence from algae fossils and biomarkers have shown that there was high lacustrine productivity during the depositional period of K_2n^1 and K_2n^2 (Yang et al., 1981; Feng et al., 2009; Zhang and Bao, 2009; Xi et al., 2012; Wang et al., 2013; Zhao et al., 2014), but they show obviously different OM abundances. The OM content is high under the anoxic condition in K_2n^1, but the OM abundance declines rapidly during K_2n^2 with its oxic environment, which suggests that even under the condition of high productivity, it still difficult to form a high OM deposit if there is not a good preservation environment for the OM.

In conclusion, the enriched $\delta^{13}C_{Ga}$ and depleted $\delta^{13}C_{hop}$ in K_2n^1 corresponds to stable water stratification and intermittent photic zone anoxia, reflecting good preservation of OM under this extreme environment, resulting in high TOC and HI. The absence of gammacerane and ^{13}C-enrichment of $\delta^{13}C_{hop}$ in K_2n^2 is consistent with aerobic and unstratified water conditions, resulting in less preservation of OM and leading to lower values of TOC and HI. As previously mentioned, the upper layer contains primarily algae and cyanobacteria produced through photosynthesis in aerobic freshwater environments, while the lower layer primarily contains anaerobic microorganism in anoxic brackish to saline water conditions in K_2n^1. For K_2n^2, the stratified water disappeared and the chemoautotrophic bacteria prevailed under brackish aerobic environments. Thus, water environments not only control the abundance of OM but also affect the microorganisms in the water.

4. Conclusions

The $\delta^{13}C$ variation of OM, steranes and hopanoids in the sediments of K_2n^{1+2} are mainly controlled by their parent material inputs and depositional environments. Through the distribution and carbon isotopic composition of each biomarker, we inferred the spatial heterogeneity of aquatic organisms in the Songliao paleo-lake. Photosynthetic algae and bacteria are dominant in the upper oxidizing water, submerged aquatic organisms grow in the upper part of the photic aerobic zone, and anoxic microorganisms, such as chemoautotrophic bacteria, predominated in the bottom water. Because the chemocline becomes shallow in K_2n^1, anaerobic populations can expand into the euphotic zone, resulting in an increase of microorganism diversity. Heterotrophic microorganism (e.g., ciliates), green sulfur bacteria and other anaerobic microorganisms lived in the chemocline, while chemoautotrophic bacteria and methanotrophic bacteria prevailed in the bottom water.

In addition, there are significant positive correlations between $\delta^{13}C$ of 4-methyl sterane and $\delta^{13}C_{Ga}$ vs water salinity. As water salinity increased, the carbon isotopic values became higher. Moreover, the $\delta^{13}C_{Ga}$ and $\delta^{13}C_{hop}$ values reflect the depth of chemocline. The enriched $\delta^{13}C_{Ga}$ and ^{13}C-depleted of $\delta^{13}C_{hop}$ in K_2n^1 indicated a shallow chemocline and intermittent photic zone anoxia, while the absence of gammacerane and ^{13}C-enrichment of $\delta^{13}C_{hop}$ can indicate a deep chemocline or aerobic conditions. Clearly, the carbon isotopic compositions of these biomarkers in the profile can be used to characterize the variations of water salinity, depth of the chemocline and diversity of water microorganisms, which are important to further study the environmental characteristics and biogeochemical processes in detail.

Acknowledgements

We thank Dr. Jiangtao Guo for assistance with GC–ir–MS and GC–MS analyses. We also thank Andrew P. Murray and two anonymous reviewers for their comments, which significantly improved the paper. This research was supported by the National Natural Science Foundation of China (NSFC) (Grant No. 41321002 and No. 4150020804).

Associate Editor—**Andrew Murray**

References

Bechtel, A., Jia, J., Strobl, S.A.I., Sachsenhofer, R.F., Liu, Z., Gratzer, R., Püttmann, W., 2012. Palaeoenvironmental conditions during deposition of the Upper Cretaceous oil shale sequences in the Songliao Basin (NE China): implications from geochemical analysis. Organic Geochemistry 46, 76–95.

Boreham, C.J., Summons, R.E., Roksandic, Z., Dowling, L.M., Hutton, A.C., 1994. Chemical, molecular and isotopic differentiation of organic facies in the Tertiary lacustrine Duaringa oil shale deposit, Queensland, Australia. Organic Geochemistry 21, 685–712.

Cabrera, L., Cabrera, M., Gorchs, R., De Las Heras, F.X.C., 2002. Lacustrine basin dynamics and organosulphur compound origin in a carbonate-rich lacustrine system (Late Oligocene Mequinenza Formation, SE Ebro Basin, NE Spain). Sedimentary Geology 148, 289–317.

Chamberlain, C.P., Wan, X., Graham, S.A., Carroll, A.R., Doebbert, A.C., Sageman, B.B., Blisniuk, P., Kent-Corson, M.L., Wang, Z., Chengshan, W., 2013. Stable isotopic evidence for climate and basin evolution of the Late Cretaceous Songliao Basin, China. Palaeogeography, Palaeoclimatology, Palaeoecology 385, 106–124.

Collister, J.W., Summons, R.E., Lichtfouse, E., Hayes, J.M., 1992. An isotopic biogeochemical study of the Green River oil shale. Organic Geochemistry 19, 265–276.

Curiale, J.A., Gibling, M.R., 1994. Productivity control on oil shale formation—Mae Sot Basin, Thailand. Organic Geochemistry 21, 67–89.

Feng, Z.H., Fang, W., Wang, X., Huang, C.Y., Huo, Q.L., Zhang, J.H., Huang, Q.H., Zhang, L., 2009. Microfossils and molecular records in oil shales of the Songliao Basin and implications for paleo-depositional environment. Science in China, Series D: Earth Sciences 52, 1559–1571.

Feng, Z.Q., Jia, C.Z., Xie, X.N., Zhang, S.C., Feng, Z.H., Timothy, A.C., 2010. Tectonostratigraphic units and stratigraphic sequences of the nonmarine Songliao basin, northeast China. Basin Research 22, 79–95.

Feng, Z.H., Fang, W., Li, Z.G., Wang, X., Huo, Q.L., Huang, C.Y., Zhang, J.H., Zeng, H.S., 2011. Depositional environment of terrestrial petroleum source rocks and geochemical indicators in the Songliao Basin. Science in China, Series D: Earth Sciences 54, 1304–1317.

Freeman, K.H., Hayes, J.M., Trendel, J.-M., Albrecht, P., 1990. Evidence from carbon isotope measurements for diverse origins of sedimentary hydrocarbons. Nature 343, 254–256.

Grice, K., Schouten, S., Peters, K.E., Sinninghe Damsté, J.S., 1998. Molecular isotopic characterisation of hydrocarbon biomarkers in Palaeocene–Eocene evaporitic, lacustrine source rocks from the Jianghan Basin, China. Organic Geochemistry 29, 1745–1764.

Grice, K., Audino, M., Boreham, C.J., Alexander, R., Kagi, R.I., 2001. Distributions and stable carbon isotopic compositions of biomarkers in torbanites from different palaeogeographical locations. Organic Geochemistry 32, 1195–1210.

Hasegawa, T., 1997. Cenomanian–Turonian carbon isotope events recorded in terrestrial organic matter from northern Japan. Palaeogeography, Palaeoclirnatology, Palaeoecology 130, 251–273.

Hasegawa, T., Pratt, L.M., Maeda, H., Shigeta, Y., Okamoto, T., Kase, T., Uemura, K., 2003. Upper Cretaceous stable carbon isotope stratigraphy of terrestrial organic matter from Sakhalin, Russian Far East: a proxy for the isotopic composition of paleoatmospheric CO_2. Palaeogeography, Palaeoclimatology, Palaeoecology 189, 97–115.

Hayes, J.M., 1993. Factors controlling ^{13}C contents of sedimentary organic compounds: principles and evidence. Marine Geology 113, 111–125.

Hayes, J.M., Freeman, K.H., Popp, B.N., Hoham, C.H., 1990. Compound-specific isotopic analyses: a novel tool for reconstruction of ancient biogeochemical processes. Organic Geochemistry 16, 1115–1128.

Hou, D., Li, M., Huang, Q., 2000. Marine transgressional events in the gigantic freshwater lake Songliao: paleontological and geochemical evidence. Organic Geochemistry 31, 763–768.

Huang, Y., Lockheart, M.J., Collister, J.W., Eglinton, G., 1995. Molecular and isotopic biogeochemistry of the Miocene Clarkia Formation: hydrocarbons and alcohols. Organic Geochemistry 23, 785–801.

Huang, Q., Chen, C., Wang, P., Han, M., Li, X., Wu, D., 1998. The late Cretaceous bio-evolution and anoxic events in the ancient lake in Songliao Basin. Acta Micropalaeontologica Sinica 15, 417–425 (in Chinese).

Huang, Y., Yang, G., Gu, J., Wang, P., Huang, Q., Feng, Z., Feng, L., 2013. Marine incursion events in the Late Cretaceous Songliao Basin: constraints from sulfur geochemistry records. Palaeogeography, Palaeoclimatology, Palaeoecology 385, 152–161.

Koch, P.L., 1998. Isotopic reconstruction of past continental environments. Annual Review of Earth and Planetary Sciences 26, 573–613.

Luo, G., Junium, C.K., Kump, L.R., Huang, J., Li, C., Feng, Q., Shi, X., Bai, X., Xie, S., 2014. Shallow stratification prevailed for ~1700 to ~1300 Ma ocean: evidence from organic carbon isotopes in the North China Craton. Earth and Planetary Science Letters 400, 219–232.

Meyers, P.A., Ishiwatari, R., 1993. Lacustrine organic geochemistry — an overview of indicators of organic matter sources and diagenesis in lake sediments. Geochimica et Cosmochimica Acta 20, 867–900.

Michael, J.D., Samuel, E.S., 1978. Influence of diet on the distribution of carbon isotopes in animals. Geochimica et Cosmochimica Acta 42, 495–506.

Neunlist, S., Rodier, C., Llopiz, P., 2002. Isotopic biogeochemistry of the lipids in recent sediments of Lake Bled (Slovenia) and Baldeggersee (Switzerland). Organic Geochemistry 33, 1183–1195.

Ourisson, G., Albrecht, P., Rohmer, M., 1979. The hopanoids: palaeochemistry and biochemistry of a group of natural products. Pure and Applied Chemistry 51, 709–729.

Pedersen, T.F., Calvert, S.E., 1990. Anoxia vs. productivity: what controls the formation of organic-carbon-rich sediments and sedimentary rocks? American Association of Petroleum Geologists Bulletin 74, 454–466.

Peters, K.E., Walters, C.C., Moldowan, J.M., 2005. The Biomarker Guide: Biomarkers and Isotopes in Petroleum Exploration and Earth History, vol. 2. Cambridge University Press, UK.

Schaffner, F.C., Swart, P.K., 1991. Influence of diet and environmental water on the carbon and oxygen isotopic signatures of seabird eggshell carbonate. Bulletin of Marine Science 48, 23–38.

Schouten, S., Klein Breteler, W., Blokker, P., Schogt, N., Rijpstra, W.I.C., Grice, K., Baas, M., Sinninghe Damsté, J.S., 1998. Biosynthetic effects on the stable carbon isotopic compositions of algal lipids: implications for deciphering the carbon isotopic biomarker record. Geochimica et Cosmochimica Acta 62, 1397–1406.

Schouten, S., van Kaam-Peters, H.M.E., Rijpstra, W.I.C., Schoell, M., Sinninghe Damsté, J.S., 2000. Effects of an oceanic anoxic event on the stable carbon isotopic composition of early Toarcian carbon. American Journal of Science 300, 1–22.

Schouten, S., Wakeham, S.G., Sinninghe Damsté, J.S., 2001. Evidence for anaerobic methane oxidation by archaea in euxinic waters of the Black Sea. Organic Geochemistry 32, 1277–1281.

Sepúlveda, J., Wendler, J., Leider, A., Kuss, H.-J., Summons, R.E., Hinrichs, K.-U., 2009. Molecular isotopic evidence of environmental and ecological changes across the Cenomanian–Turonian boundary in the Levant Platform of central Jordan. Organic Geochemistry 40, 553–568.

Sinninghe Damsté, J.S., Schouten, S., 1997. Is there evidence for a substantial contribution of prokaryotic biomass to organic carbon in Phanerozoic carbonaceous sediments? Organic Geochemistry 26, 517–530.

Sinninghe Damsté, J.S., Kenig, F., Koopmans, M.P., Koster, J., Schouten, S., Hayes, J.M., de Leeuw, J.W., 1995. Evidence for gammacerane as an indicator of water column stratification. Geochimica et Cosmochimica Acta 59, 1895–1990.

Song, Z., Qin, Y., George, S.C., Wang, L., Guo, J., Feng, Z., 2013. A biomarker study of depositional paleoenvironments and source inputs for the massive formation of Upper Cretaceous lacustrine source rocks in the Songliao Basin, China. Palaeogeography, Palaeoclimatology, Palaeoecology 385, 137–151.

Summons, R.E., Powell, T.G., 1986. Chlorobiaceae in Paleozoic seas revealed by biological markers, isotopes and geology. Nature 319, 763–765.

van Kaam-Peters, H.M.E., Schouten, S., de Leeuw, J.W., Sinninghe Damsté, J.S., 1997. A molecular and carbon isotope biogeochemical study of biomarkers and kerogen pyrolysates of the Kimmeridge Clay Facies: palaeoenvironmental implications. Organic Geochemistry 27, 399–422.

Volkman, J.K., 2003. Sterols in microorganisms. Applied Microbiology and Biotechnology 60, 496–506.

Volkman, J.K., Zhang, Z., Xie, X., Qin, J., Borjigin, T., 2015. Biomarker evidence for *Botryococcus* and a methane cycle in the Eocene Huadian oil shale, NE China. Organic Geochemistry 78, 121–134.

Wang, L., Song, Z., Yin, Q., George, S.C., 2011. Paleosalinity significance of occurrence and distribution of methyltrimethyltridecyl chromans in the Upper Cretaceous Nenjiang Formation, Songliao Basin, China. Organic Geochemistry 42, 1411–1419.

Wang, C., Feng, Z., Zhang, L., Huang, Y., Cao, K., Wang, P., Zhao, B., 2013. Cretaceous paleogeography and paleoclimate and the setting of SKI borehole sites in Songliao Basin, northeast China. Palaeogeography, Palaeoclimatology, Palaeoecology 385, 17–30.

Xi, D., Wan, X., Feng, Z., Li, S., Feng, Z., Jia, J., Jing, X., Si, W., 2011. Discovery of Late Cretaceous foraminifera in the Songliao Basin: evidence from SK-1 and implications for identifying seawater incursions. Chinese Science Bulletin 56, 253–256.

Xi, D., Li, S., Wan, X., Jing, X., Huang, Q., Colin, J.P., Wang, Z., Si, W., 2012. Late Cretaceous biostratigraphy and paleoenvironmental reconstruction based on non-marine ostracodes from well SK1 (south), Songliao Basin, northeast China. Hydrobiologia 688, 113–123.

Yang, W.L., Li, Y.K., Gao, R.Q., Guo, Q.F., 1981. The types and evolution of parent organic matter in petroleum source rocks of Songliao Lacustrine Oil Basin. Science in China 8, 1000–1008 (in Chinese).

Zhang, Y., Bao, L., 2009. Cretaceous Phytoplankton Assemblages from Songke Core-1, North and South (SK-1, N and S) of Songliao Basin, Northeast China. Acta Geologica Sinica (English Edition) 83, 868–874.

Zhang, Y., Jiang, A., Sun, Y., Xie, L., Chai, P., 2012. Stable carbon isotope compositions of isoprenoid chromans in Cenozoic saline lacustrine source rocks from the Western Qaidam Basin, NW China: source implications. Chinese Science Bulletin 57, 1013–1023.

Zhao, J., Wan, X., Xi, D., Jing, X., Li, W., Huang, Q., Zhang, J., 2014. Late Cretaceous palynology and paleoclimate change: evidence from the SK1 (South) core, Songliao Basin, NE China. Science China Earth Sciences 57, 2985–2997.